The 2025 World Congress on
Advances in Structural Engineering and Mechanics (ASEM25)
BEXCO, Busan, Korea, August 11-14, 2025

Development of a Control System for Automating Cable Inspection Robots on Cable-Stayed Bridges

*Kyogo Mizuashi[1)] and Shinobu Kakehashi[2)]
Toshihiro Okumatsu[3)], Shozo Nakamura[4)], and Takafumi Nishikawa[5)]

[1),3), 4), 5)] *Nagasaki University, Nagasaki, Japan*
[2)]*Chodai Co., Ltd. Fukuoka, Japan*
[1)] bb54124209@ms.nagasaki-u.ac.jp

abstract

The cable-stayed bridge cable inspection robot was developed by Kakehashi. (Kakehashi. 2022) is operated with partially automatic control and manual control. The current challenge is to improve the accuracy of PID control, which calculates the amount of control from the deviation from the target speed; PID control has three coefficients: proportional, integral, and derivative, and the amount of control is calculated from these coefficients and the error between the current speed and the target speed. In the experiment, the behavior of the machine was checked using four different patterns of changes in the PID control coefficients. Based on the time history of the velocity, the coefficients with the smallest velocity amplitude and shortest elapsed time were considered to have the appropriate response. However, even this appropriate response did not result in smooth behavior during ascent. In the future, we plan to increase the number of patterns of PID control coefficients and conduct statistical evaluation by scoring the range of motion and the number of hovering times.

1. Introduction

In response to accidents caused by aging social infrastructure, such as the Sasago Tunnel accident on the Chuo Expressway, the Ministry of Land, Infrastructure, Transport and Tourism (MLIT) has designated 2013 as the “First Year of Social Capital Maintenance” (MLIT White Paper 2023), and has since formulated the “Basic Plan for Infrastructure Longevity Improvement” and “MLIT Infrastructure Longevity Plan (Action Plan)” and has been working on priority measures. Since then, the “Basic Plan for Infrastructure Longevity Extension” and the “Ministry of Land, Infrastructure and Transport Infrastructure Longevity Plan (Action Plan)” have been formulated and priority measures have been taken.

[1)] Graduate Student
[3), 4)] Professor
[5)] Associate Professor

On the other hand, road bridges are aging and the need for their maintenance and management is increasing. As of July 2025, approximately 320 cable-stayed bridges have been constructed throughout Japan (Ministry of Land, Infrastructure, Transport and Tourism Chronological Table of Road Statistics 2024). As shown in Figure 1.1, cable-stayed bridges are extremely important components that support bridge girders with diagonally stretched cables (cable-stays) from the main tower and balance the entire bridge. Periodic inspections of bridges are required by law, with the first inspection to be conducted within two years after the bridge is placed in service, and the second and subsequent inspections to be conducted once every five years. However, traffic control is required during inspections, resulting in cost losses due to traffic congestion and other problems, as well as ensuring the safety of workers at heights. In addition, it is desirable to inspect the exterior of cables in conjunction with the periodic inspection of bridges once every five years. However, the height that can be inspected by a high clearance vehicle on a bridge is generally limited to about 30 m. Since the main towers of cable-stayed bridges are often 30 m or higher and are installed at high locations, close-up visual inspection has not been possible so far. Therefore, as shown in Fig. 1.2, visual inspections have been conducted from the road surface or from an elevated vehicle at a distance. Whenever possible, special elevated work is performed by workers at heights.

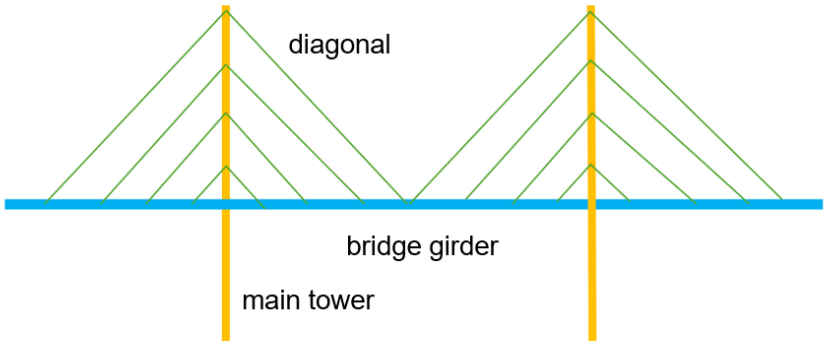

Fig.1.1 Schematic of cable-stayed bridge

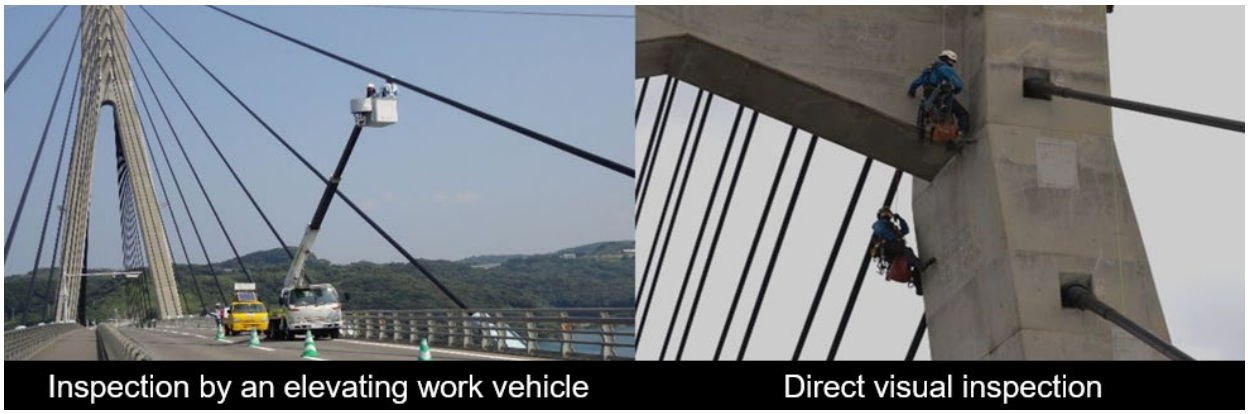

Fig.1.2 Conventional inspection of cable-stayed bridge cables

As shown in Figure 1.3, cable-stayed bridge cables often have a structure in which steel wires are bundled and protected by a sheath made of polyethylene or other material. In the worst case, major measures such as cable replacement are required. Under these circumstances, cable damage such as that shown in Figure 1.4 has been discovered, and there is an urgent need to develop a system that enables safe and rapid inspection in close proximity. Against this background, an inspection robot for cable-stayed bridge cables has recently been developed, as shown in Figure 1.5, which can indirectly visually inspect the cable surface by taking pictures of the cable surface from the upper end to the lower end with four cameras from four directions.

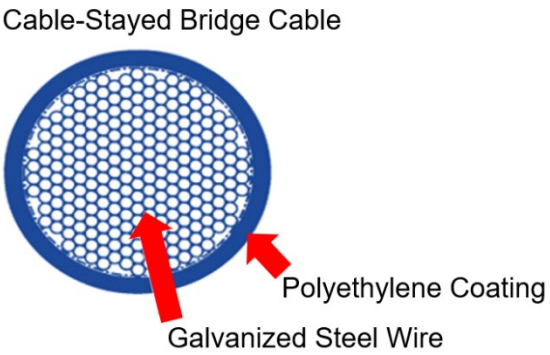

Fig.1.3 Example of cable-stayed bridge cable structure

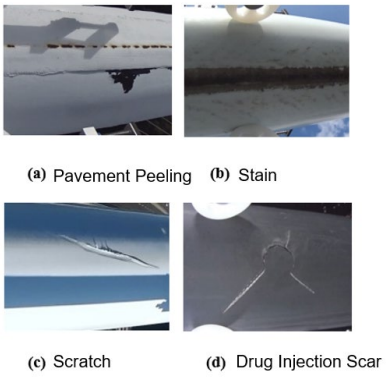

Fig.1.4: Example of cable-stayed bridge cable damage

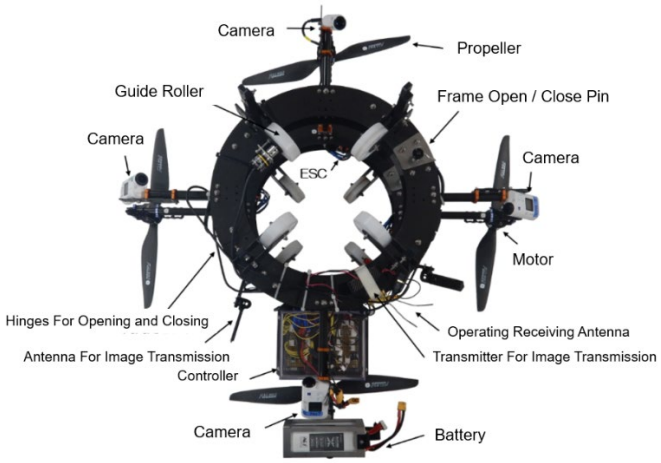

Fig.1.5 Example of cable-stayed bridge cable inspection robot

In industries such as construction and transportation, where a shortage of workers is a growing concern, the use of advanced IT technology is expected to greatly improve productivity in the future. In addition, the reduction of work around heavy machinery and work at heights will ensure safety, and women and the elderly are also expected to play an active role. In recent years, development toward automation and remote control of robots has been underway in construction and infrastructure maintenance.

The cable-stayed bridge cable inspection robot developed by Ladai et al. (Ladai et al. 2022) uses four cameras to capture images of the cable surface from four directions. It is equipped with a propeller and travels along the cable using the propulsion of the propeller. Currently, the robot is operated by partially automatic control and manual control. However, improving the accuracy of PID control, which calculates the control amount based on the deviation from the target speed, has become an issue. The objectives of this study are to confirm the operation of the equipment used and to optimize the coefficients used in PID control for fully automatic control.

2. Fully automated robot inspection system under development

The cable-stayed bridge cable inspection robot itself has already been developed. In this chapter, we present an overview of the fully automated system and the configuration of the program.

2.1 Overview of the Fully Automated System

Figure 2.1 shows the configuration of the machine used in this study. High-power LiPo batteries are used to drive the entire machine. On the other hand, a mobile battery is used for the SD card for data storage to improve system stability by decentralizing the power supply.

The aircraft is equipped with a rotary encoder for speed control and a laser distance sensor for turning control near the main tower (at the top of the cable). Based on the

speed data acquired by the rotary encoder, PID control is used to control the movement of the aircraft. As shown in Equation (1), the motor speed is calculated by taking into account the error e(t) between the target speed and the current speed and the proportional, integral, and derivative components. During control cycle t, the proportional component uses the current error as it is, the integral component calculates the accumulated error to date, and the derivative component calculates the rate of change of the error. The motor speed is obtained by combining these components and is reflected in the motor as an output value.

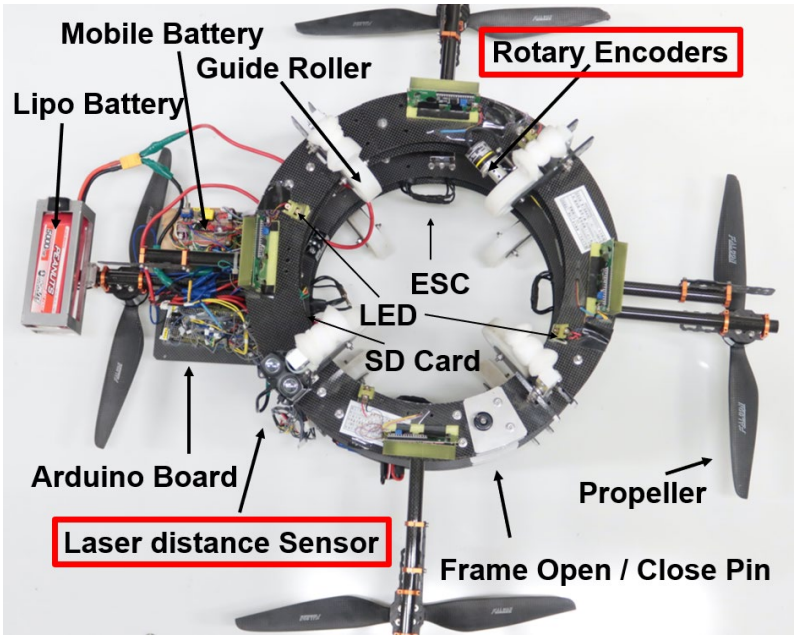

Fig. 2.1 Configuration of external equipment on the aircraft

$$K_P e(t) + K_i \int e(t)\,dt + K_d \frac{de(t)}{dt} \quad (1)$$

2.2 Program Structure

Figure 2.2 shows the structure of the automatic program under development. The control system performs the initial settings for interfacing with its external devices and acquires the measured values of the rotary encoder and laser distance sensor. The amount of change in the laser distance sensor is used to determine the direction of movement, with a positive value indicating a downward movement and a negative value indicating an upward movement. A stepwise target speed is selected according to the results. As shown in Table 2, there are five target speed steps for ascending and six for descending, and each step is sequentially switched based on the state of the direction of movement, distance, or position. To calculate the current speed, the distance traveled is calculated from the change between the current distance acquired by the rotary encoder and the previous distance, and the speed is obtained by dividing

the distance traveled by the time elapsed since the previous time. The elapsed time is measured in milliseconds, and the control cycle t is approximately 10 to 50 ms. The PID control has three coefficients: proportional coefficient Kp, integral coefficient Ki, and derivative coefficient Kd. The proportional coefficient Kp increases the speed of following the target speed by adjusting the control amount in proportion to the error, but too large a coefficient may cause fluctuations in the system output values. The integration factor Ki adjusts the control amount based on the accumulation of errors to eliminate steady-state deviations. However, too large a factor may cause system instability. The derivative coefficient Kd adjusts the amount of control based on the rate of change of the error and serves to suppress system oscillations. However, it also makes the system more sensitive to noise. The proportional term P is calculated by multiplying the velocity error by the proportionality factor Kp, and the integral term I and derivative term D are calculated using this term. The integral term I is obtained by integrating the error over time as the cumulative amount of the velocity error. The derivative term D is the change in error divided by time and is used to adjust the response to abrupt changes. The control amount is calculated by summing these three terms, and control processing is performed to keep the output within the upper and lower limits set for this control amount. Based on the limited control value, a pulse width modulation signal that controls the average power supplied is generated and output to the motor. Finally, the error history is updated for the next and subsequent controls, and the control process and values are recorded on an SD card and stored as a log.

Tab. 2 Example of target speed

Terms Distance of Rotary Encoders：A Distance of Laser distance Sensor：B	Target Speed （descent）	条件 Distance of Rotary Encoders：：A Distance of Laser distance Sensor：B	Target Speed （ascent）
B < 1.0 m and Speed ≧ 0 m/s	- 0.1 m/s	A < 1.0 m and Speed≧ 0 m/s	0.2 m/s
B ＜ 1.0 m and	- 0.1 m/s	1.0 m ≦ A and 5.0 m ≦ B	0.5 m/s

Speed＜0 m/s		and Speed≧ 0 m/s	
1.0 m ≦ B ＜ 2.0 m and Speed＜0 m/s	- 0.2 m/s	3.0 m ≦ B ＜ 5.0 m and Speed≧ 0 m/s	0.3 m/s
1.0 m ≦ B and 5.0 m ＜ B and Speed＜0 m/s	- 0.3 m/s	2.0 m ≦ B ＜ 3.0 m and Speed≧ 0 m/s	0.2 m/s
2.0m ≦ B and 5.0 m ＜ A and Speed＜0 m/s	- 0.2 m/s	1.0 m ≦ B ＜ 2.0 m and Speed≧ 0 m/s	0.1 m/s
2.0 m ≦ A and A ＜ 5.0 m and 2.0m ≦ B and Speed＜0 m/s	- 0.1 m/s		

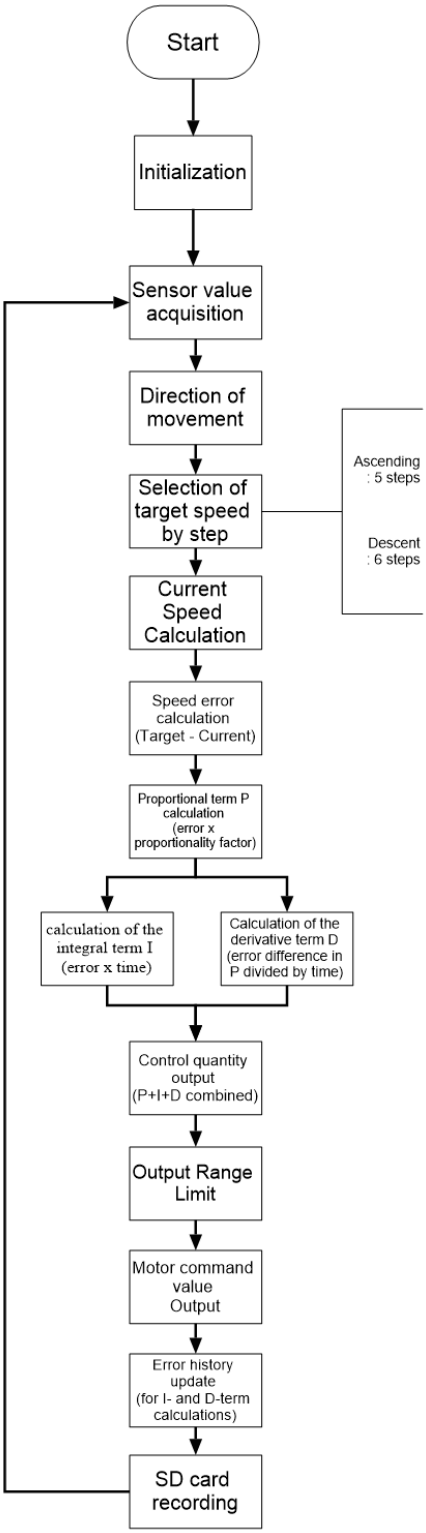

Fig. 2.2 Structure of the automatic control program at this stage

3. Checking external devices

We checked whether the rotary encoder and laser distance sensor required for automatic control have sufficient functions.

3.1 Checking the rotary encoder

The rotary encoder is a sensor used to measure the moving speed of the aircraft, and the acquired data is used to control the rotation speed of the motor. Using a 4-m void pipe that simulates a cable-stayed bridge cable, the machine without a propeller was moved by hand a total of three times under automatic control. The measured distance traveled was compared with the value obtained by the rotary encoder to confirm the results. The actual measured distance was 3.35 m, whereas the data acquired three times was 3.34 m. This indicates that the rotary encoder was not operating properly. This confirmed that the rotary encoder was working properly.

3.2 Checking the laser distance sensor

The results of checking the laser distance sensor are shown in Figure 3. The distance obtained when the laser sensor was separated from the wall by 2 m from 0 to 17 m was checked. As shown in the figure, it was confirmed that the distance from the wall was acquired without any problem.

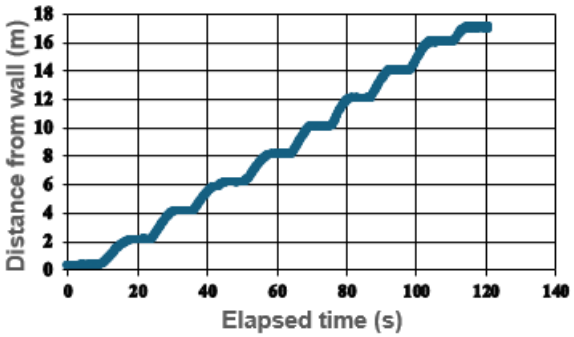

Fig. 3 Checking the laser distance sensor

4. checking automatic control in the aircraft and changing PID control coefficients

Full automatic control was verified using an 8-m void pipe simulating a cable-stayed bridge cable. Figure 4.1 shows the experimental situation. The first PID control coefficients used in this experiment were Kp: 12, Ki: 1, and Kd: 12 (case 1). Based on the results of the actual operation, several coefficient patterns were considered. Table 4 shows a selection of four representative patterns with distinctly different behavior trends. The selection of coefficients was adjusted step by step while evaluating the

effects of the proportional, integral, and derivative components on the system response, and does not cover all combinations.

Tab. 4 Patterns for changing PID control coefficients

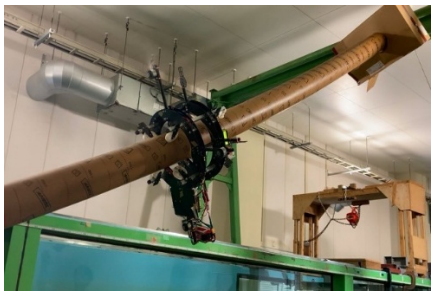

	Kp	Ki	Kd
case1	12	1	12
case2	48	0.5	60
case3	36	2	72
case4	24	2	24

Fig.4.1 Automatic control in an indoor experiment

Figure 4.2 shows the velocity error vs. elapsed time during ascent in cases 1 through 4. The control performance of case 4 was evaluated from the viewpoint of control performance, and case 4 showed the best control characteristics among cases 1 to 4. case 4 showed a balanced convergence behavior with a relatively small fluctuation range of speed error and a response time that was neither excessively fast nor too slow, which was optimal from the viewpoint of reducing the load on the motor and energy efficiency. This means that the operating characteristics were close to optimal from the viewpoints of motor load reduction and energy efficiency. On the other hand, a few issues remain in case 4, such as a sudden stop of the machine in a fixed position at a specific moment and a lack of smooth velocity change. This may be due to inadequate vibration suppression by the differential component or the response to abrupt error changes when switching target speeds.

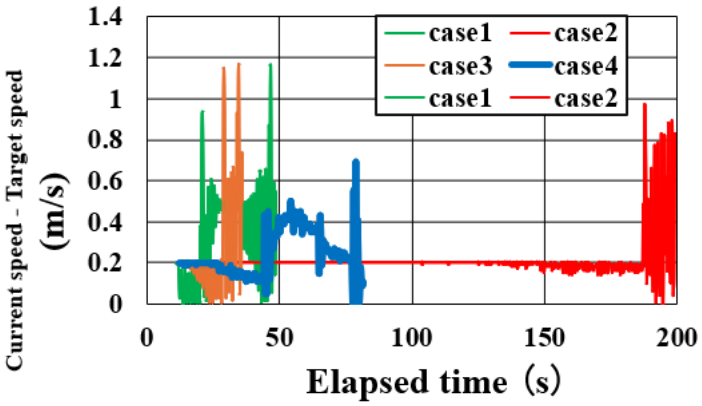

Fig.4.2 Time variation of velocity error for each PID control coefficient

5. Conclusion

In this study, the PID control of the cable-stayed bridge cable inspection robot was improved to optimize the coefficients used in the PID control, which is related to the operation check of each external device and speed control. 24, Ki: 2, and Kd: 24 showed the control characteristics with the lowest vibration, appropriate response time, and stability. On the other hand, there were some cases where abrupt changes were observed when the aircraft was hovering, indicating that there is room for further improvement.

In the future, we plan to increase the number of PID control coefficient patterns and statistically evaluate the control results, such as the range of motion and the number of times of hovering, to verify the control performance more objectively and precisely. In addition, by combining the optimization of coefficients through simulation and fine-tuning through experimentation, we aim to derive the optimal PID coefficients and achieve smooth and stable movement control.

References

Kakehashi, S., Fujiki, T., Nakamura, S., Yamamoto, I. and Nakashima, S. (2022), “Development of a cable inspection robot for cable-stayed bridges and its applications to existing bridges”, *Steel Construction Engineering., Vol.29,* No.113. (in Japanese)